Journal of Rock Mechanics and Geotechnical Engineering 17 (2025) 7007–7022

Contents lists available at ScienceDirect

Journal of Rock Mechanics and Geotechnical Engineering

journal homepage: www.jrmge.cn

Full Length Article

Thermal effect on shear and compressive behaviors of rock fractures: Cases of sandstone and granite

Abdel Kareem Alzo'ubi [a,*], Mahmoud Alneasan [b]

[a] Civil Engineering Department, College of Engineering, Abu Dhabi University, Al Ain, United Arab Emirates
[b] Geotechnical Engineering Department, College of Civil Engineering, Tishreen University, Latakia, Syria

A R T I C L E I N F O

Article history:
Received 29 August 2024
Received in revised form
25 November 2024
Accepted 2 December 2024
Available online 5 July 2025

Keywords:
Sedimentary sandstone
Igneous granite
Thermal treatment
Joint shear behavior
Joint compressive behavior
Direct shear test

A B S T R A C T

The growing demand for geothermal energy exploration and deep engineering projects necessitates a deeper understanding of rock behavior under extreme thermal conditions. This study investigates the effect of thermal treatment on the shear behavior of sedimentary sandstone and igneous granite, which are abundant in the Earth's crust. Direct shear tests were conducted on rock joints at room temperature (RT), 250 °C, and 500 °C. The results show that the joints in sandstone and granite exhibit improved compressive and shear strength up to a temperature threshold of 200 °C–350 °C, followed by significant weakening beyond this range. This study investigated key parameters, including normal and shear stiffness, maximum joint closure, peak and residual shear strengths, internal friction angle, dilation angle, and cohesion. The compressive behavior of both rock types followed a modified Bandis's equation. The peak shear strength followed Patton's bilinear and Jaeger's nonlinear failure criteria more accurately than the Mohr–Coulomb criterion. The results of this study provide valuable insights into the temperature-dependent behavior of sandstone and granite joints under compressive and shear loads, and their interoperation was strongly dependent on the mineralogical and structural components of the two rock types. These results have advanced our understanding of the temperature-dependent behavior of rock fractures, improving the safety of underground structures under thermal effects.

1. Introduction

Rocks, in their natural state, experience a wide range of temperatures depending on location, depth, and geological history. These temperature variations can significantly influence the mechanical behavior of rocks, often resulting in the alteration of their physical and mechanical properties. Understanding the behavior of rocks under different temperature conditions is essential in various engineering applications. Examples include underground mines (Rathnaweera et al., 2018), nuclear waste repositories (Hudson et al., 2001), and geothermal energy extraction sites (Jiang et al., 2024). As engineering projects go deeper, the thermal effect becomes increasingly important due to an increase in the surrounding temperature with depth, at an average rate of 3 °C–5 °C per 100 m (Rimi et al., 2012). In such scenarios, mechanical stability and rock mass preservation are crucial. Quantifying the temperature's effect on rocks' strength and deformation is essential for the successful design and operation of these projects.

Extensive research efforts have been made to investigate the temperature-induced changes in the mechanical behavior of rocks. Laboratory experiments, including uniaxial compression (Lu et al., 2017; Zhang et al., 2017; Pan et al., 2023), triaxial compression (Ma et al., 2020; Meng et al., 2020; Zhou et al., 2024), tension (Alneasan and Alzo'ubi, 2022; Alzo'ubi and Alneasan, 2022; Su et al., 2022), and shear tests (Tang, 2020; Alneasan and Alzo'ubi, 2023; Bi et al., 2023; Alzo'ubi et al., 2024) are commonly carried out to analyze the effects of temperature on the strength parameters of rocks. The effect of temperature on the behavior of rock joints and their shear strength has been a topic of great interest in geological and geotechnical engineering. Several studies have been conducted to investigate the thermal treatment effect on the shear behavior of intact and fractured rocks, and different regimes for temperature-dependent shear behavior in various rock types have been

* Corresponding author.
E-mail address: abdel.alzoubi@adu.ac.ae (A.K. Alzo'ubi).
Peer review under responsibility of Institute of Rock and Soil Mechanics, Chinese Academy of Sciences.

https://doi.org/10.1016/j.jrmge.2024.12.035
1674-7755/

concluded. Tang et al. (2020) studied the effect of thermal treatment in the temperature range from room temperature (RT) to 800 °C on the basic friction angle of jointed marble, sandstone, and granite. They showed that the basic friction angle of sandstone and granite increases with increasing temperature, while it is inversely proportional to the temperature in marble. Moreover, some researchers have investigated the effect of thermal treatment on the shear behavior of jointed (Zhang et al., 2019) and intact (Bi et al., 2023) sandstone, and jointed (Zhao et al., 2019) and intact (Zhu et al., 2021; Chen et al., 2023) granite. They concluded a declining trend in the shear strength parameters with increasing temperature. However, other researchers observed two regimes for temperature-dependent shear behavior in the intact sandstone (Yang et al., 2017; Yin et al., 2021; Liu et al., 2022), and jointed (Tang, 2020; Zhai et al., 2022) and intact granite (Zhang et al., 2018; Ma et al., 2020; Yang et al., 2022). They pointed out that the shear strength parameters can improve with increasing temperature up to a certain temperature threshold, followed by slight or significant deterioration when that threshold is exceeded. Tang et al. (2019) investigated the effect of thermal treatment on intact marble and concluded that the cohesion first increased with increasing temperature from 20 °C to 300 °C, and then decreased as the treatment temperature further increased to 600 °C. However, the relationship between the internal friction angle and the temperature was the opposite of that of the cohesion. Meng et al. (2020) observed that the internal friction angle of intact limestone increases with temperature up to 400 °C, after which it decreases as the temperature continues to increase. However, cohesion showed an opposite trend with temperature increase. It should be noted that the rates of improvement and deterioration in the shear strength parameters, as well as the temperature threshold variation, can be attributed to the mineralogical and structural compositions of each rock.

In this study, we use two rock types: sandstone and granite, as they are two widely utilized rock types in engineering applications due to their abundance and favorable mechanical properties. Sandstone is the second most common sedimentary rock after shale, constituting about 20%–25% of the sedimentary rocks in the Earth's crust (Boggs, 2011). Granite is one of the igneous rocks that form the majority of the first 20–25 km of the Earth's crust (70%–80%) (Singh et al., 2014). Understanding the behavior of these rocks under different temperature conditions is, therefore, particularly important. Based on the literature, previous studies on the shear strength of rocks under temperature influences predominantly explored intact rocks, with some examining rock fractures. Each study focused on a specific rock type and addressed certain parameters regarding fracture behavior under shear stress. Some investigations dealt with saw-cut joints, which do not reflect the natural roughness of rock joints. Additionally, some studies emphasized ultimate shear strength at the expense of residual shear strength, and not all examined the impact of temperature on dilation behavior during shearing. Accordingly, further research is necessary to accurately quantify the effect of temperature and thermal treatment on the compressive and shear behavior of sandstone and granite fractures by considering most parameters governing this behavior, such as maximum joint closure, peak and residual shear strengths, normal and shear stiffness, residual strength ratio, dilation angle, internal friction angle, and cohesion. This study focuses on the effect of temperature on the compression behavior of a single continuous joint in these two rock types. The governing equations that govern the linear and nonlinear behavior of sandstone and granite joints under compression and shear as a function of thermal treatment temperature are also examined.

2. Mineral composition of the studied rocks

The present study includes two main types of igneous and sedimentary rocks: granite and sandstone. The mineral composition determined by preparing microscopic thin sections is shown in Fig. 1. Fig. 1a shows that the sandstone mainly consists of 35% plagioclase (Pl), 29% quartz (Q), 14% iron oxide (IO), 13% clay minerals (Cl), 7% calcite (Ca), and 2% voids (V). Fig. 1b shows that the granite mainly consists of 70% plagioclase, 25% quartz, and less than 5% orthoclase and amphibole. It can be noted that plagioclase is the main constituent mineral in sandstone and granite, followed by quartz. The percentage of plagioclase and quartz in the sandstone is 100% and 16% greater, respectively, compared to those in the granite. In addition, the grain size distribution was analyzed using ImageJ and @Risk software, as shown in Fig. 1c for sandstone and Fig. 1d for granite. These figures show that grain sizes range from 30.2 μm to 185.4 μm in sandstone and from 278 μm to 1092 μm in granite. This indicates that the average grain size in granite is 6.35 times greater than in sandstone.

3. Experimental procedure

The experimental procedure in this study includes sample preparation, selection of joints of similar roughness, thermal treatment of selected samples, and a direct shear test on control samples at RT and thermally treated samples.

3.1. Sample preparation

Fig. 2 shows the procedure used in this study to prepare granite and sandstone joints. First, a sufficient number of prismatic samples were cut from the same rock block (Fig. 2a). To ensure sample homogeneity, all prismatic samples were then subjected to P-wave detection to avoid the effect of rock heterogeneity on the final direct shear results. Subsequently, artificial tensile joints were formed in the prismatic samples using the techniques to develop tensile joints in prismatic or cubic rock samples as described by Tang (2020), Zhai et al. (2022), and Zhao et al. (2019) (Fig. 2b). The prismatic samples were placed between two high-strength metal jaws and compressed to the failure point. This technique produced many undesired joints with wavy surfaces or a non-straight fracture path between the upper and lower loading jaws. As a result, a large number of artificial joints had to be made to select the best ones (fit for our experiment) in terms of the fracture path's straightness and the surfaces' roughness. Nine perfect joints of each type of rock were obtained by creating about 70 joints in sandstone and 40 in granite. To enhance sample preparation, the prismatic samples must have parallel surfaces to minimize parallelism error and apply the load perpendicularly to both surfaces. The edges of the upper and lower jaws should be polished and smooth for uniform load transmission to the rock sample. Additionally, increasing the loading or strain rate can lead to straighter joints. Next, the flattest 6 cm × 6 cm was determined on each joint as the shear zone (Fig. 2d), and the rock samples were cut to the required dimensions. After that, all joints with dimensions of 6 cm × 6 cm were checked according to the roughness condition explained in the next section, and the joints that did not meet this condition were excluded. In this study, 9 sandstone and 9 granite samples were subjected to thermal treatment and direct shear test. These samples were prepared in the concrete molds shown in Fig. 2e for the direct shear device. Fig. 2f shows the finished sandstone and granite samples after their preparation in the concrete molds.

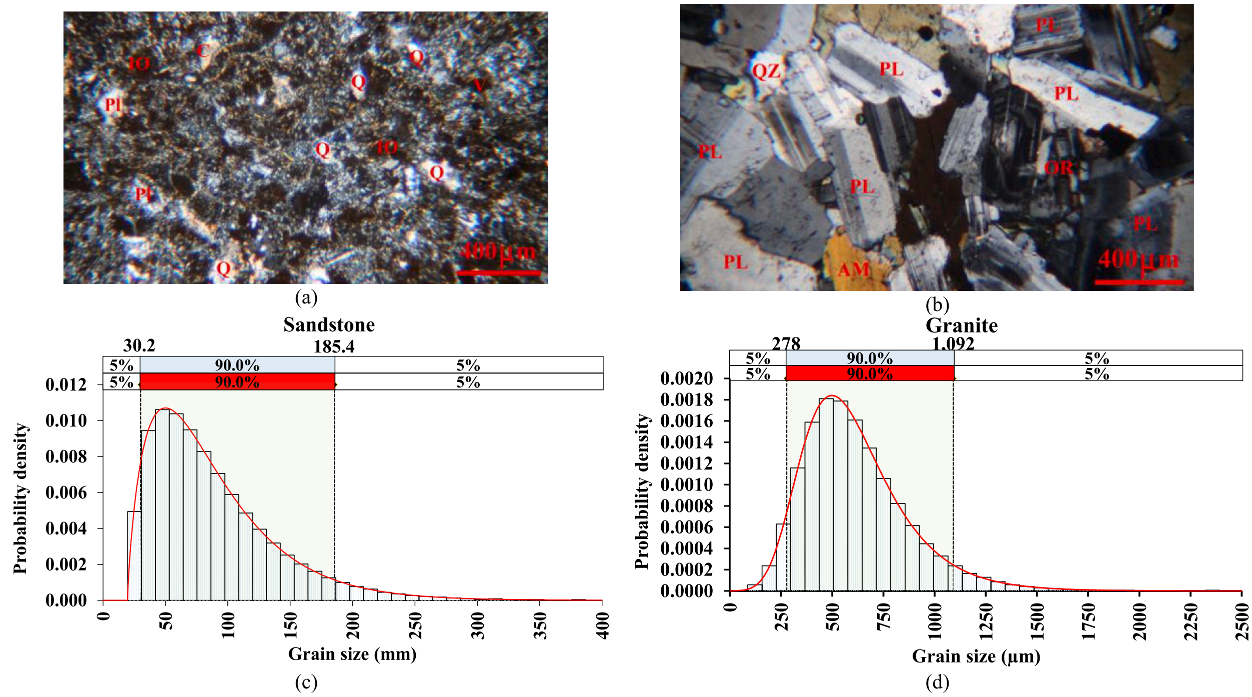

Fig. 1. Mineral composition and grain size distribution of the sandstone (a, c) and granite (b, d) used in this study.

Fig. 2. Sample preparation: (a) Prismatic blocks of sandstone and granite; (b) The method used to generate artificial tensile joints; (c) The formed joints in prismatic samples; (d) Determination of the flattest 6 cm × 6 cm area on each joint; (e) Preparation of the resulting samples in the concrete molds of the direct shear device; and (f) The final samples adopted in this study for direct shear test.

3.2. Evaluation of the joint roughness

One of the most important variables influencing the behavior of a joint during shear and compression tests is its roughness. As a result, the chosen joints for each kind of rock must be similar in terms of roughness coefficient to properly investigate the effect of thermal treatment on the shear behavior of sandstone and granite joints. Each joint's shear direction was identified, as illustrated in Fig. 3, and the roughness coefficient can be calculated along this direction using the following equation (Akhavan and Rajabipour, 2012):

$$R = \frac{1}{\lambda}\sum(|Z_{\text{REF}} - Z_{\text{FP}}|\cos\alpha) \tag{1}$$

where λ is the segment length along which the roughness is evaluated, and $\lambda = 6$ cm in our case; α is the slope of this segment, and $\alpha = 0°$ in this study; Z_{FP} is the Z-coordinate of joint asperities, which were measured every 0.05 mm along the segment length λ; Z_{REF} is the Z-coordinate of the red reference line shown in Fig. 3, and Z_{REF} is constant for all points on the joint surface and can be calculated as an average of Z_{FP}.

To choose 18 samples, a preliminary evaluation of some sandstone and granite joints was made with the naked eye. The roughness coefficient was calculated for 15 samples of each rock type, and the results are shown in Fig. 4. The average roughness coefficient, R_{av}, was calculated for the 15 joints. Those joints for which the roughness coefficient differed from the average value by more than 4% were excluded. Fig. 4a and b shows that only 9 sandstone joints and 10 granite joints met the roughness condition. Accordingly, 9 samples of sandstone joints and 9 of granite joints were selected for testing at RT and after thermal treatment at 250 °C and 500 °C. Three samples of each rock type were tested under each temperature.

3.3. Thermal treatment

Temperature is considered one of the most important environmental factors that affect rocks' mineral and structural composition. At the mineralogy level, an increase in temperature beyond a certain limit can lead to irreversible chemical and physical changes in the constituent minerals of the rock. For example, the α/β quartz transition can occur at a temperature threshold of 573 °C. After this temperature, quartz undergoes a reversible change and transforms from its natural form (α-quartz) to its new form (β-quartz) (Fraser, 1986). At the structural level, the α/β quartz transition is accompanied by a substantial increase in the material volume due to the rise in intergranular thermal fractures (Griffiths et al., 2017). This phenomenon can lead to an increase in the fracture width (Johnson et al., 1978; Nasseri et al., 2007).

As demonstrated above, the determination of the maximum thermal treatment temperature is closely related to the mineral composition of the tested rock. Mineralogical studies have indicated that sandstone and granite have a high percentage of quartz, 29% in sandstone and 25% in granite. The maximum thermal treatment temperature is related to the research objective. In this study, the effect of α/β quartz transition and its volumetric expansion on the direct shear behavior of sandstone and granite is not one of the objectives of the current study. Therefore, the maximum temperature adopted in this study was 500 °C, and an average temperature of 250 °C was adopted between RT and 500 °C to show how the shear behavior of sandstone and granite changes when the temperature increases from RT to 500 °C.

Thermal treatment on sandstone and granite samples was conducted using the furnace shown in Fig. 5a, following heating and cooling paths illustrated in Fig. 5b. Initially, the rock samples were gradually heated at a low heating rate of 4 °C/min until the desired temperature was reached. Subsequently, the rock samples were exposed to the desired temperature for 24 h. Finally, the furnace was turned off, and the rock samples were naturally cooled at a low cooling rate of 1 °C/min. It should be noted that the heating and cooling rates in this study are sufficiently low as to cause thermal shock in the rock samples.

3.4. Testing method

The direct shear test on sandstone and granite joints was conducted in this study according to the ASTM standard method (ASTM D5067–16(2021), 2021) to measure the shear strength under constant normal stress. The test was performed in two stages: (1) the consolidation stage, in which the joint was vertically loaded to a maximum normal stress of 6 MPa (Fig. 6a); and (2) the shear stage (Fig. 6b), in which the joint was sheared under three constant normal stresses of 0.5 MPa, 1 MPa, and 1.5 MPa, following the methodology of multiple shear tests with repositioning (Fig. 6c). The apparatus used in this study with side accessories is depicted in Fig. 6e. It can be observed that the sandstone and granite joints were sheared under relatively low normal stress. The main reason for selecting the aforementioned normal stresses in the shear stage is to prevent the complete crushing of small asperities on joint surfaces, thereby enabling the study of the effect of thermal treatment on joint asperities in the sliding and shear stages (Patton's perspective). The details related to the direct shear tests conducted in this study are summarized in Table 1.

4. Results and discussion

This study primarily explores how thermal treatment influences the behavior of sandstone and granite joints under compressive and shear loads. For the compressive load analysis,

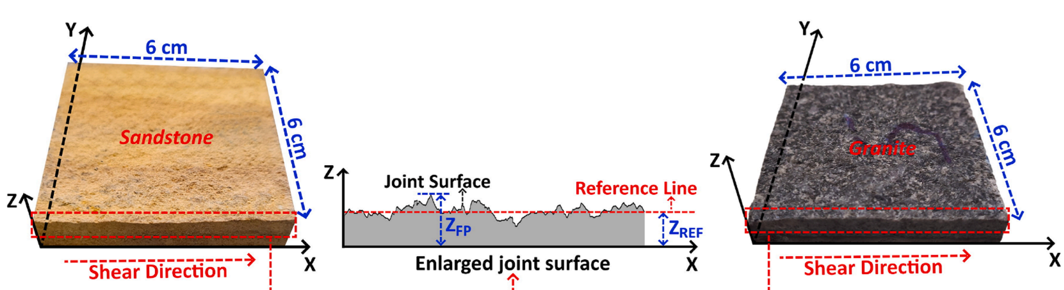

Fig. 3. Evaluation of joint roughness.

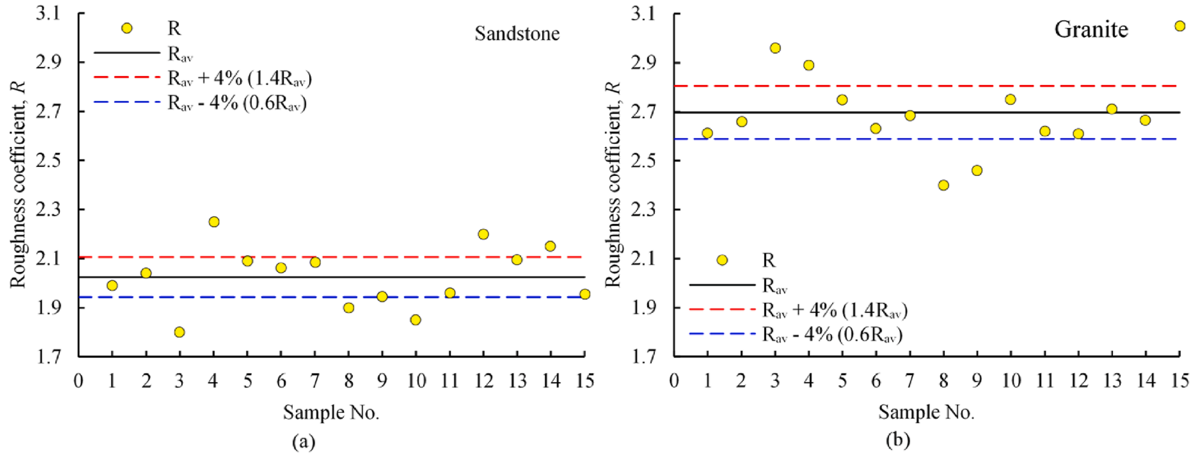

Fig. 4. Evaluation and selection of rock joints adopted in this study for thermal treatment and direct shear test based on roughness coefficient: (a) Sandstone and (b) granite.

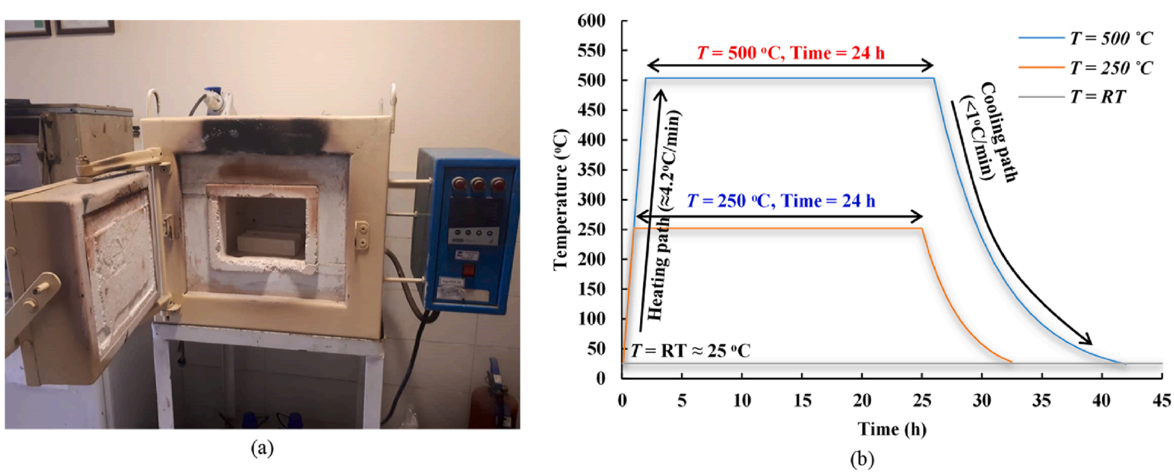

Fig. 5. Thermal treatment: (a) The furnace used in this study; and (b) Heating and cooling paths used for thermal treatment.

key parameters such as maximum joint closure and normal stiffness were measured and examined. Additionally, equations were formulated to describe the relationship between applied normal stress (σ_n) and normal displacement (δ_n). For the shear load analysis, parameters including peak and residual shear strengths, shear stiffness, dilation angle, drop stress, internal friction angle, and cohesion were considered.

4.1. Thermal treatment effect on the joints' behavior under compression

The effect of thermal treatment on the σ_n-δ_n curves of sandstone and granite joints before and after thermal treatment is shown in Fig. 7. As illustrated in the figure, raising the temperature from RT to 250 °C significantly enhances the joint strength of both rock types under compression. The maximum joint closure is defined as the highest vertical displacement achieved as the normal stress continuously increases, indicating that the joint has fully closed. This parameter corresponds to an infinite slope on the σ_n-δ_n curve. It is determined experimentally by plotting the σ_n-δ_n curve and identifying the vertical section of this curve that approaches an infinite slope. As demonstrated in Fig. 7, the maximum joint closure (δ_m) decreases as the temperature increases from RT to 250 °C. This effect on maximum joint closure for both rock types is individually depicted in Fig. 8a. Notably, the average maximum joint closure for both rock types is almost identical across the three temperatures examined. The relationship between maximum joint closure and temperature is represented by a second-order polynomial curve. The lowest point on the curve indicates the temperature threshold at which the behavior of maximum joint closure shifts from decreasing to increasing. Specifically, the maximum joint closure for sandstone and granite joints decreases by approximately 37.5% and 38.8%, respectively, after thermal treatment at 250 °C, and then increases by about 138.8% and 144.3%, respectively, after treatment at 500 °C. The temperature threshold for this behavioral change is 215 °C.

4.1.1. Thermal treatment effect on the normal stiffness

Normal stiffness is an important parameter in rock mechanics for understanding joint behavior under compression. It plays a significant role in analytical and numerical simulations of joint behavior in rock masses, particularly when considering environmental factors like temperature in deep engineering projects. The normal stiffness is determined as the slope of the σ_n-δ_n curve at any given point. Once the governing equation for the relationship between applied normal stress and normal displacement is formulated, the normal stiffness can be found by differentiating this equation with respect to normal displacement ($K_n = d\sigma_n/d\delta_n$). It was observed that the relationship between σ_n and δ_n in sandstone and granite joints, both before and after thermal treatment,

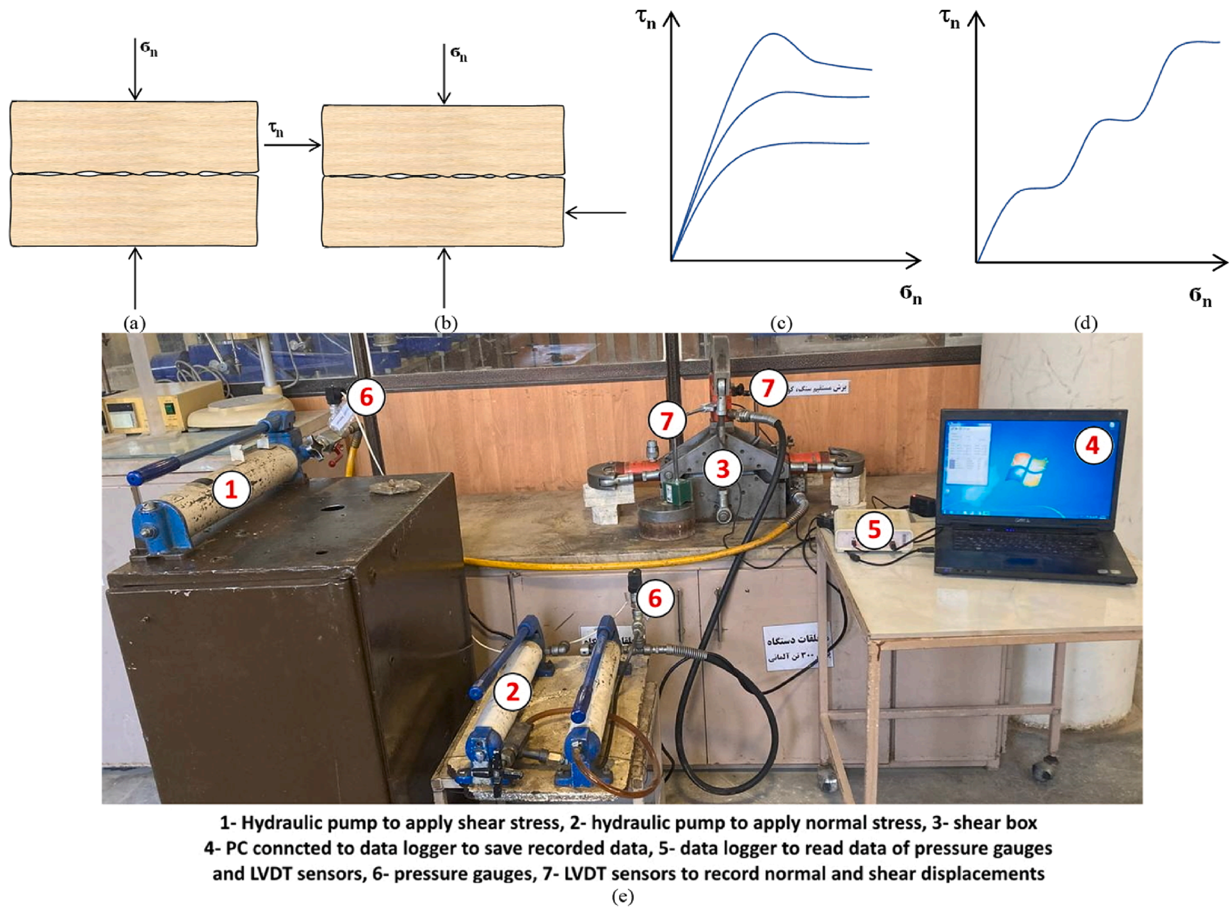

Fig. 6. Testing method: (a) Consolidation stage; (b) Shear stage; (c) Multiple shear tests with repositioning; (d) Multiple shear tests without repositioning; and (e) The apparatus used in this study with side accessories.

aligns with a partially modified version of the equation proposed by Bandis et al. (1983). The original equation (Eq. (2)) accurately predicts the σ_n-δ_n curve for normal stresses between 0 MPa and 3 MPa. However, for $\sigma_n > 3$ MPa, the original equation predicts an σ_n-δ_n curve that is significantly different from the experimental one. By incorporating an exponential parameter (b) in the original equation, the slightly modified equation (Eq. (3)) gives predictions close to the experimental data.

Table 1
Conditions and specifications followed for straight shear tests in this study.

Test parameter	Description/Value
Rock type	Sandstone, granite
Test stages	Two stages: consolidation and shear stages
Maximum stress in the consolidation stage	6 MPa
Sample dimensions	6 cm × 6 cm
Applied normal stress	0.5 MPa, 1 MPa, 1.5 MPa
Shear stress measurement	Conducted at constant normal stress levels
Roughness condition	Selected samples with similar roughness
Temperature condition	RT, 250 °C, 500 °C
Number of samples per condition	3 (per rock type, per temperature)
Shear stage	Multiple shear tests with repositioning
Test equipment	A direct shear device, a P-wave detection system

$$\sigma_n = \frac{k_o \delta_n}{1 - \delta_n/\delta_m} \tag{2}$$

$$\left.\begin{aligned} \sigma_n &= \frac{k_o \delta_n}{(1 - \delta_n/\delta_m)^b} \\ k_o^{SD} &= -2.17 \times 10^{-4} T^2 + 1.11 \times 10^{-1} T + 5.37 \\ k_o^{GR} &= -5.7 \times 10^{-5} T^2 + 2.44 \times 10^{-2} T + 8.17 \\ b^{SD} &= 1.62 \times 10^{-6} T^2 - 9.3 \times 10^{-4} T + 0.282 \\ b^{GR} &= -3.74 \times 10^{-8} T^2 + 1.88 \times 10^{-4} T + 0.255 \\ \delta_m^{SD} \approx \delta_m^{GR} &= 2.27 \times 10^{-6} T^2 - 9.79 \times 10^{-4} T + 0.228 \end{aligned}\right\} \tag{3}$$

$$K_n = \frac{d\sigma_n}{d\delta_n} = -\frac{k_o[1 + (b-1)\delta_n/\delta_m]}{(\delta_n/\delta_m - 1)(1 - \delta_n/\delta_m)^b} \tag{4}$$

where k_o and b are the empirical constants as a function of temperature; and the superscripts "SD" and "GR" denote the sandstone and granite, respectively. The predicted results of Eq. (3) are shown with dashed lines in Fig. 7. A high degree of agreement between experimental (continuous lines) and predicted (dashed lines) results can be observed in this figure. The equation for normal stiffness was derived by differentiating Eq. (3) with respect to δ_n,

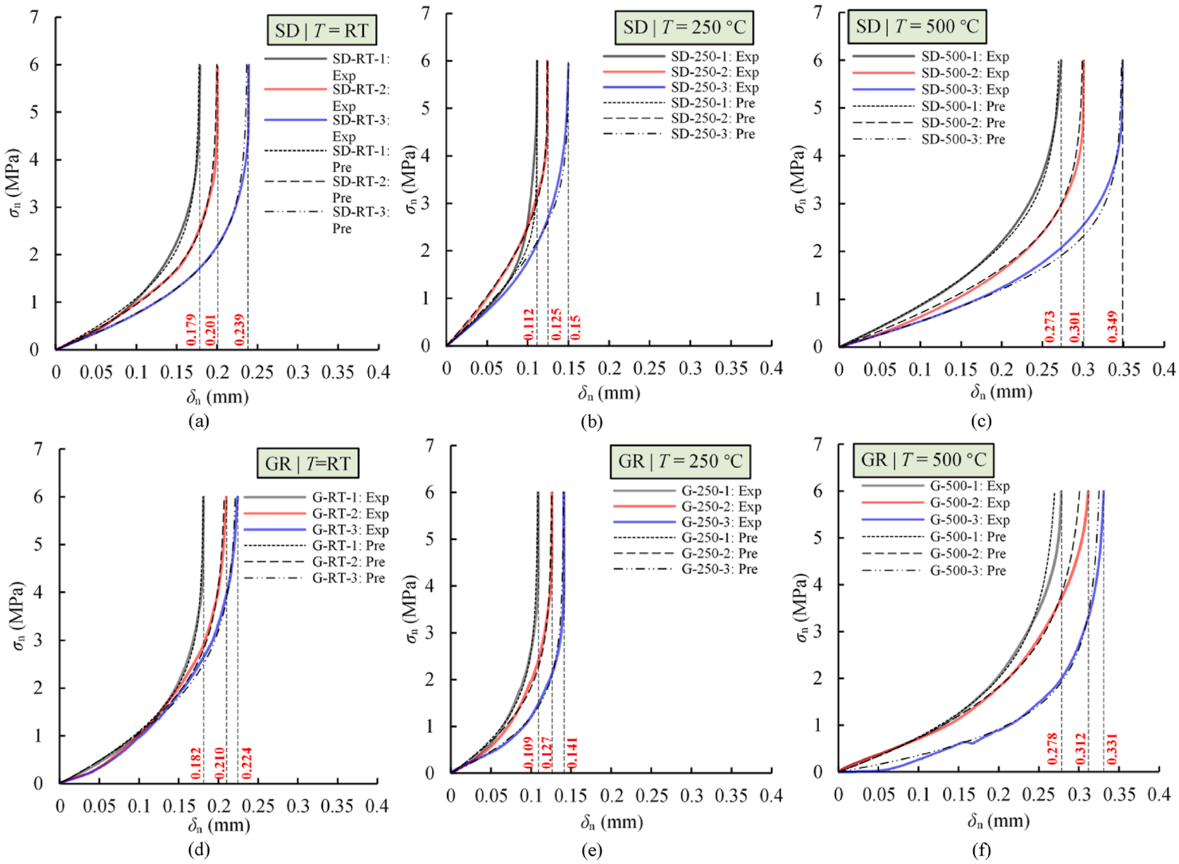

Fig. 7. Thermal treatment effect on the behavior of (a–c) sandstone and (d–f) granite joints under compressive stress. Exp: Experimental results; Pre: Predicted results.

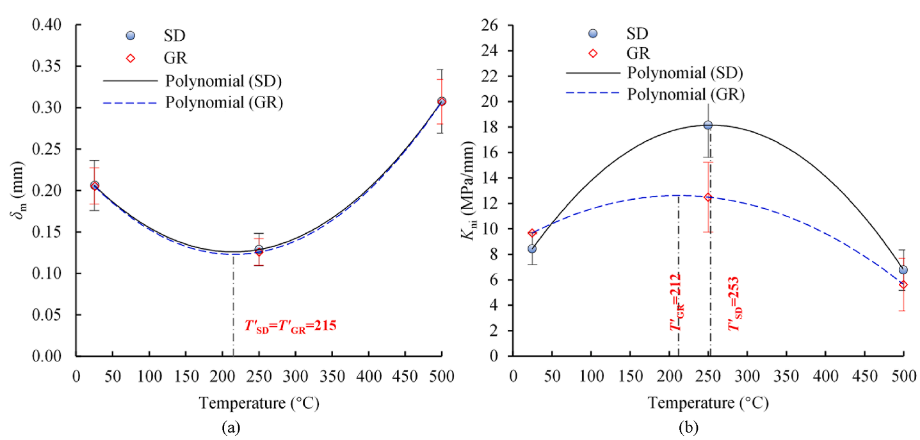

Fig. 8. The effect of thermal treatment on the (a) maximum joint closure and (b) initial normal stiffness.

resulting in Eq. (4). The initial normal stiffness (K_{ni}) for all joints was calculated within a normal displacement range of 0–0.05 mm, and the effect of temperature on this parameter is illustrated in Fig. 8b. It can be observed that K_{ni} behaves in two distinct ways as the temperature increases from RT to 500 °C. At RT, granite joints exhibited a slightly higher K_{ni} than sandstone joints. After thermal treatment at 250 °C, the K_{ni}^{SD} for sandstone joints increased by approximately 115.1%, resulting in a 1.45-fold increase in comparison to that of granite joints (K_{ni}^{GR}). Following thermal treatment at 500 °C, the initial normal stiffness of sandstone and granite joints decreased by about 62.7% and 55%, respectively. In addition, the temperature thresholds at which sandstone and granite joints change their K_{ni} behavior are 253 °C and 212 °C, respectively.

The impact of thermal treatment on the behavior of rock joints under compression has been scarcely covered in the literature. Jiang et al. (2024) examined this effect on granite joints within a temperature range from RT to 300 °C. They considered key parameters such as joint closure and normal stiffness, and found that joint closure decreases with increasing normal stress and temperature. In contrast, the normal stiffness increases with both temperature and normal stress. Our findings for sandstone and granite align with those reported by Jiang et al. (2024), as shown in Fig. 8, where δ_m decreases and K_{ni} increases with temperature up to 250 °C. Conversely, Liu et al. (2023) discovered that the normal stiffness of fractured granite decreases steadily as the temperature rises from RT to 600 °C.

4.2. Thermal treatment effect on the joints' behavior under shear

The effect of thermal treatment and applied normal stress on the shear stress–shear displacement (τ_s-δ_s) curves of sandstone and granite joints are presented in Fig. 9. To better illustrate the impact of thermal treatment on joint behavior, the shear results for various treatment temperatures are plotted together in Fig. 9. A single representative curve for each temperature was included in Fig. 9 to demonstrate how temperature influences the τ_s-δ_s curves, as displaying all curves simultaneously would make it difficult for the reader to distinguish between them. As shown in Fig. 9, for the two rock types, the τ_s-δ_s curves move upward as the temperature increases from RT to 250 °C, indicating an improvement in the shear strength. However, after thermal treatment at 500 °C, the τ_s-δ_s curves move downward and the area beneath them decreases. This behavior shows a deterioration in the shear strength of sandstone and granite joints after thermal treatment at the highest temperature. In addition, the normal displacement δ_n was measured during the direct shear test to evaluate the effect of thermal treatment on the dilation angle. Fig. 10 shows the typical τ_s-δ_s and δ_n-δ_s curves for one of the sandstone samples (SD-250-1-1), along with the parameters that can be obtained from these curves and discussed. The following sections provide a detailed discussion of the impact of thermal treatment on each parameter.

4.2.1. The effect of thermal treatment on the peak and residual shear strengths

Fig. 11 illustrates the peak and residual shear strengths as a function of temperature and applied normal stress. Several important conclusions about the effect of thermal treatment on these two parameters can be drawn from this figure. Firstly, the peak shear strength of granite joints (τ_P^{GR}) is greater than that of sandstone joints (τ_P^{SD}), and the difference between them increases as the temperature rises from RT to 250 °C, and then decreases as the temperature rises to 500 °C. This trend is also evident in the residual shear strength in the two rock types. Secondly, the peak shear strength of both sandstone and granite joints exhibits two regimes when the temperature increases from RT to 250 °C and 500 °C. An increase in peak shear strength can be observed following thermal treatment at 250 °C; however, this strength declines after thermal treatment at 500 °C. This behavior was observed by some researchers regarding the effect of thermal treatment on the peak shear strength of sandstone (Bi et al., 2023) and granite (Jiang et al., 2024; Wang et al., 2024a) joints. Thirdly, the temperature threshold at which the tested joints change their τ_P-related behavior (under three normal stresses) ranges from 272 °C to 316 °C in sandstone and from 223 °C to 238 °C in granite.

The residual shear strength of granite joints behaves similarly to the peak shear strength with increasing temperatures from RT to 250 °C and 500 °C. This strength improves with increasing temperature from RT to a temperature threshold of 222 °C–252 °C, after which it deteriorates. In contrast, the residual shear strength of sandstone joints appears to be less affected by the thermal treatment temperature than that of granite joints. Under the three applied normal stresses, the τ_R^{SD} slightly decreases with increasing temperature from RT to 250 °C and 500 °C.

4.2.2. The effect of thermal treatment on the residual strength ratio τ_R/τ_P

The residual strength ratio is the ratio of residual to peak shear strength (τ_R/τ_P). It is an important parameter for describing the post-peak behavior of brittle and ductile joints (Meng et al., 2021). As this ratio increases, the residual shear strength approaches the peak shear strength and the joint behaves in a ductile manner, and vice versa when the residual strength ratio decreases. The residual strength ratio is paramount in geophysics because it describes the fault behavior. According to Rice (1996), a scenario with a large strength drop τ_R-τ_P, low τ_R/τ_P, describes a strong but brittle fault, strong because of the high τ_P but brittle because of the low τ_R.

Fig. 12 shows the effect of temperature on the τ_R/τ_P ratio of sandstone and granite joints under three applied normal stresses. This figure shows two opposite behaviors for the temperature effect on the τ_R/τ_P of sandstone and granite joints. For sandstone joints, the τ_R/τ_P decreases with increasing temperature from RT to a temperature threshold between 250 °C and 500 °C, and then increases after that threshold is exceeded. The brittleness degree of sandstone joints firstly increases with increasing temperature to a threshold of 329 °C under $\sigma_n = 0.5$ MPa, 295 °C under $\sigma_n = 1$ MPa, and 338 °C under $\sigma_n = 1.5$ MPa. Then it decreases when the temperature exceeds these thresholds. On the other hand, the results for granite joints indicated that the brittleness degree of these joints decreases with increasing temperature to a threshold of 338 °C under $\sigma_n = 0.5$ MPa, 204 °C under $\sigma_n = 1$ MPa, and 209 °C under $\sigma_n = 1.5$ MPa, and then increases when the temperature surpasses the mentioned thresholds.

4.2.3. The effect of thermal treatment on the shear stiffness

To precisely compare the results between sandstone and granite joints, as shown in Fig. 10, the secant shear stiffness K_s for all joints was calculated from the origin (0, 0) to the point at 50% of the peak shear strength (δ_s, 50% of τ_P). Fig. 13 illustrates the effect of temperature on the shear stiffness of sandstone and granite joints under the three applied normal stresses. It shows that the shear stiffness follows a similar behavior to the normal stiffness as the treatment temperature rises from RT to 250 °C and 500 °C. The shear stiffness of sandstone joints reaches its maximum value at a temperature threshold of 239 °C, 254 °C, and 258 °C under σ_n of 0.5 MPa, 1 MPa, and 1.5 MPa, respectively. The temperature thresholds for granite joints are 248 °C, 279 °C, and 288 °C as the normal stress increases from 0.5 MPa to 1 MPa and then to 1.5 MPa. In addition, the ratio of shear stiffness between granite and sandstone joints (K_s^{GR}/K_s^{SD}) ranges from 1.3 to 1.6 under different temperatures and normal stress conditions. This observed behavior regarding the effect of thermal treatment on shear stiffness in sandstone and granite joints aligns with the findings in the literature. Yin et al. (2021) reported an improvement in sandstone shear stiffness up to around 250 °C, followed by a decline beyond that temperature. Chen et al. (2020) and Jiang et al. (2024) found that granite shear stiffness peaked at temperature thresholds of 230 °C and 100 °C, respectively, and decreased as the temperature rose above these thresholds.

4.2.4. The effect of thermal treatment on the dilatancy

The effect of thermal treatment on dilation behavior was examined by calculating the dilation angle (ψ). This angle was determined as the slope of the normal displacement versus shear displacement curve at the peak shear strength (Fig. 10). Fig. 14 illustrates the dilation angle for both sandstone and granite joints as a function of temperature and normal stress. The dilation angle in granite joints is significantly greater than that in sandstone joints, particularly after thermal treatment at about 250 °C. Fig. 14 also

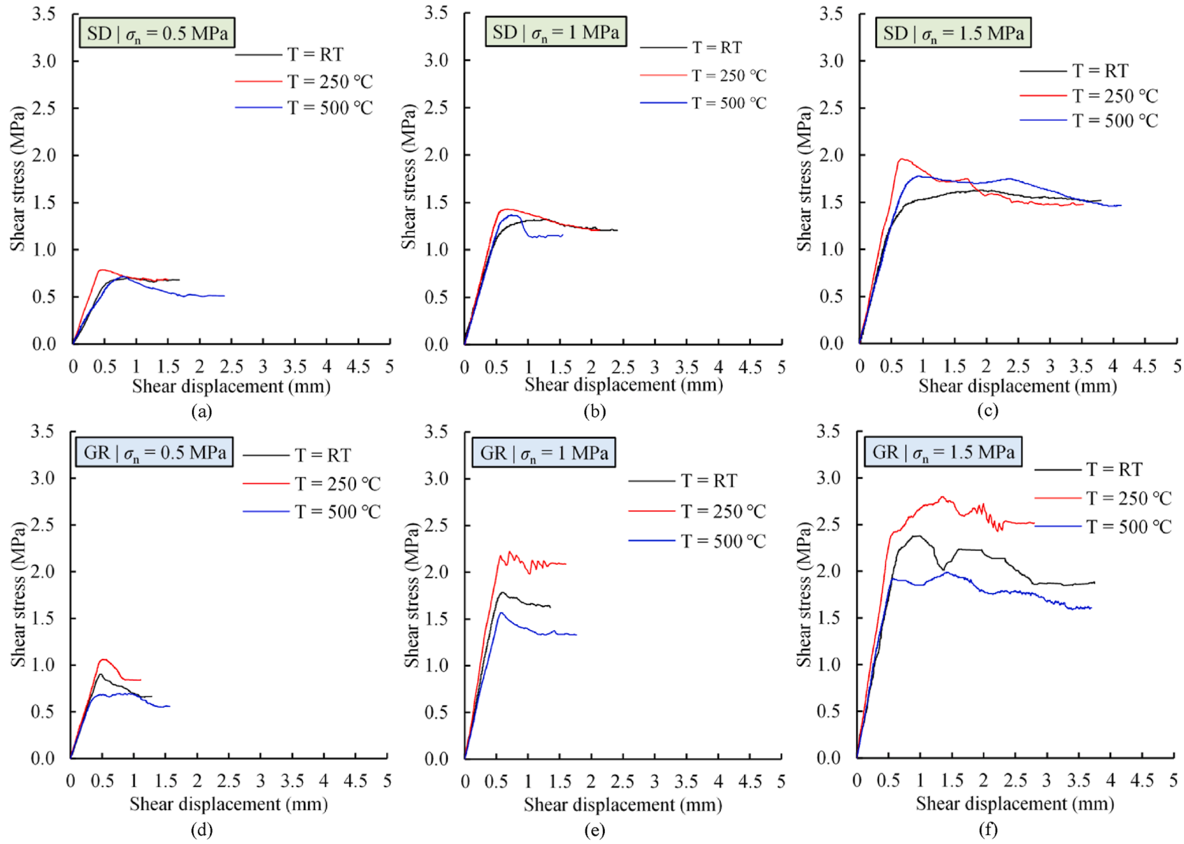

Fig. 9. The effect of thermal treatment on τ_s-δ_s curves of (a–c) sandstone and (d–f) granite joints.

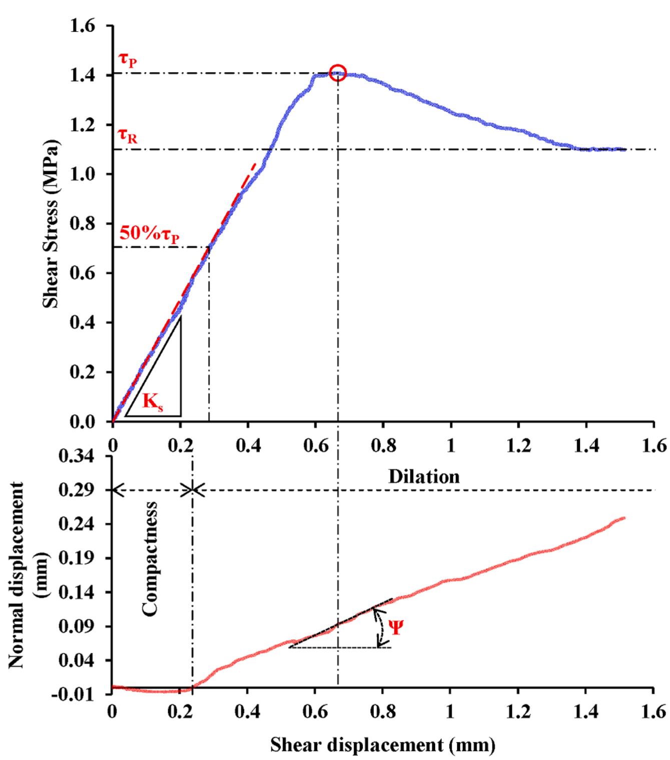

Fig. 10. Typical τ_s-δ_s and δ_n-δ_s curves for one of the sandstone samples (SD-250-1-1) along with the parameters that can be extracted from these curves.

shows that the dilation angle behavior mirrors that of normal and shear stiffness and peak and residual shear strengths under thermal treatment. In granite joints, the dilation angle measured under σ_n = 0.5 MPa, 1 MPa, and 1.5 MPa increases by about 41.2%, 165.2%, and 52.5%, respectively, after thermal treatment at 250 °C, and then it decreases by about 79.4%, 67.6% and 41.6%, respectively, after thermal treatment at 500 °C. Some researchers, such as Zhai et al. (2022), have observed this behavior and demonstrated the evolution of the dilation angle of intact and healed granite joints with increasing temperature under different normal stresses. They concluded that the dilation angle remained unchanged or slightly increased before the temperature threshold of 400 °C, and then dramatically decreased after the temperature threshold was exceeded.

Regarding the effect of thermal treatment on the dilation angle of sandstone joints, Fig. 14 shows that under σ_n of 0.5 MPa, 1 MPa, and 1.5 MPa, the dilation angle increases by about 228.1%, 48.2%, and 18.6%, respectively, after thermal treatment at 250 °C. However, it decreases by about 48.6%, 53.7%, and 25.6%, respectively, after thermal treatment at 500 °C. Regarding this behavior, Yin et al. (2021) found that the dilatancy of sandstone increases up to a temperature threshold of 400 °C, showing that the terminal normal displacement at a shear displacement of 10 mm initially increased and then decreased with the temperature *T*, peaking at 400 °C.

Thermal treatment significantly influences the dilation behavior of both sandstone and granite joints. Up to 250 °C, the dilation angle increases as the mechanical properties of both rock types improve. Enhancing the mechanical properties of the asperities between the joint surfaces encourages sliding on their

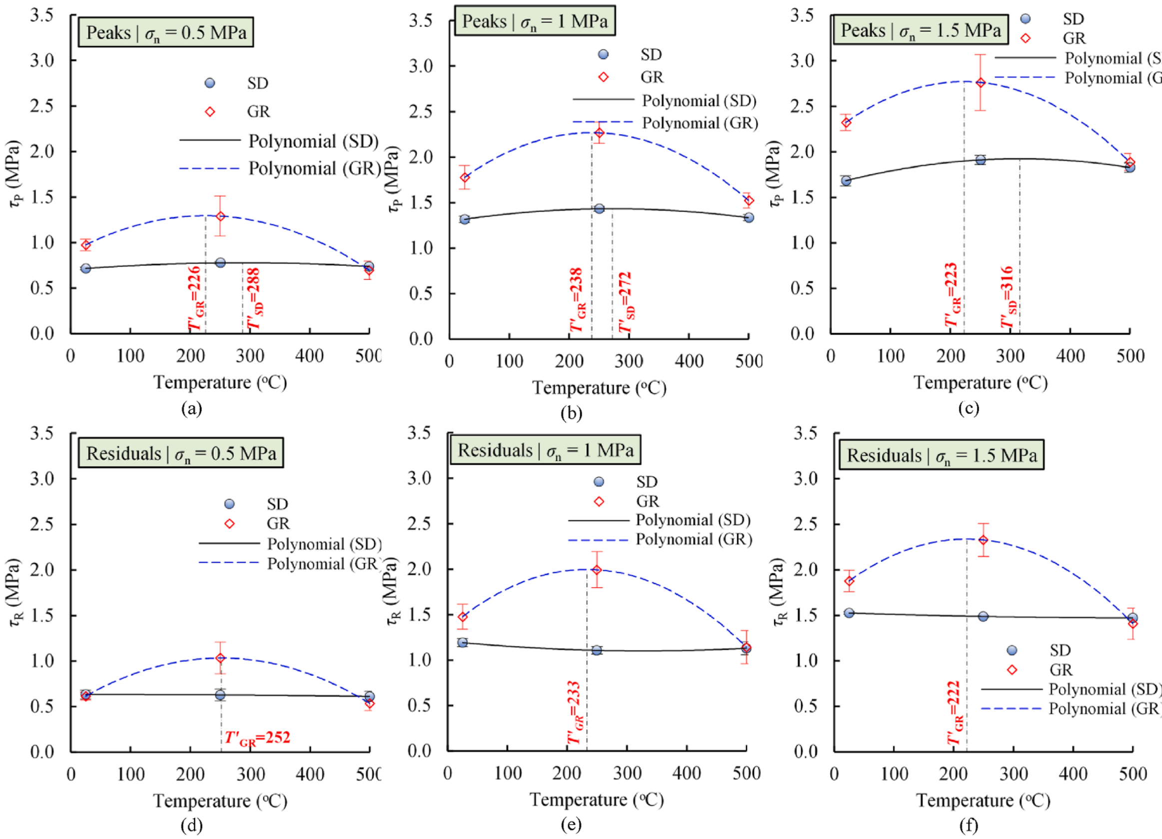

Fig. 11. The effect of thermal treatment on the (a–c) peak and (d–f) residual shear strengths.

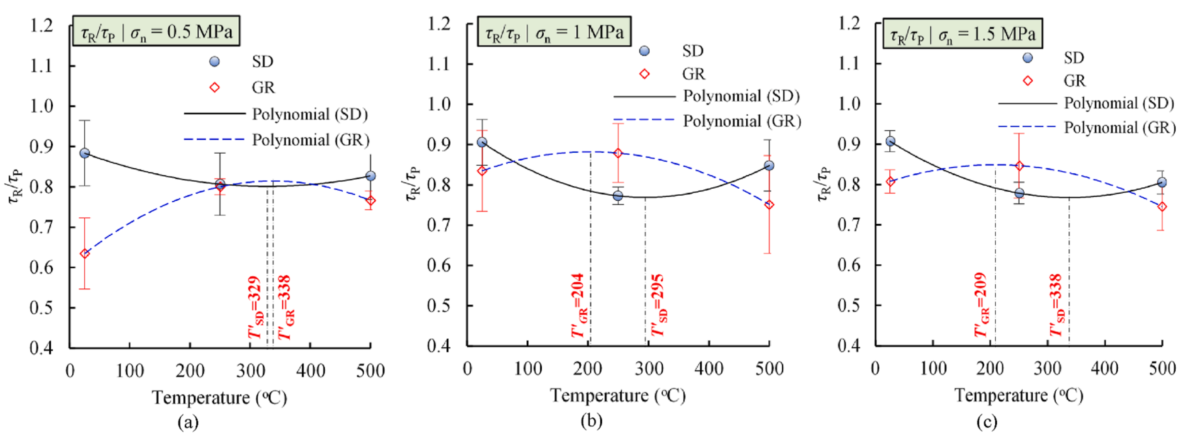

Fig. 12. The effect of thermal treatment on the residual strength ratio τ_R/τ_P.

surfaces instead of shearing them, which increases vertical displacement during shearing and ultimately raises the dilation angle. Once the temperature surpasses 250 °C, however, thermal microcracks merge into larger fractures, and the mechanical properties of sandstone and granite deteriorate. This reduces the rocks' ability to dilate under shear stress. This marks a shift from brittle to more ductile behavior, particularly in granite due to its higher quartz content. At temperatures higher than 250 °C, certain asperities may shear rather than slide along their surfaces during direct shear testing. As a result, the surface becomes smoother, minimizing the dilation angle by minimizing the vertical displacement. Additionally, since coarser grains experience more substantial microcracking, the larger grain size in granite probably contributes to its greater dilation angle compared to sandstone. On average, granite grains are 6.35 times larger than sandstone grains. As grain size increases, the asperities on the joint surfaces become more noticeable, making sliding on these raised asperities easier. Once sliding begins, the dilation angle increases immediately, which improves normal displacement under shearing. These results imply that grain size and mineral composition significantly influence the dilation behavior of rock joints, with a critical temperature threshold of around 250 °C-300 °C, beyond which dilation begins to decrease.

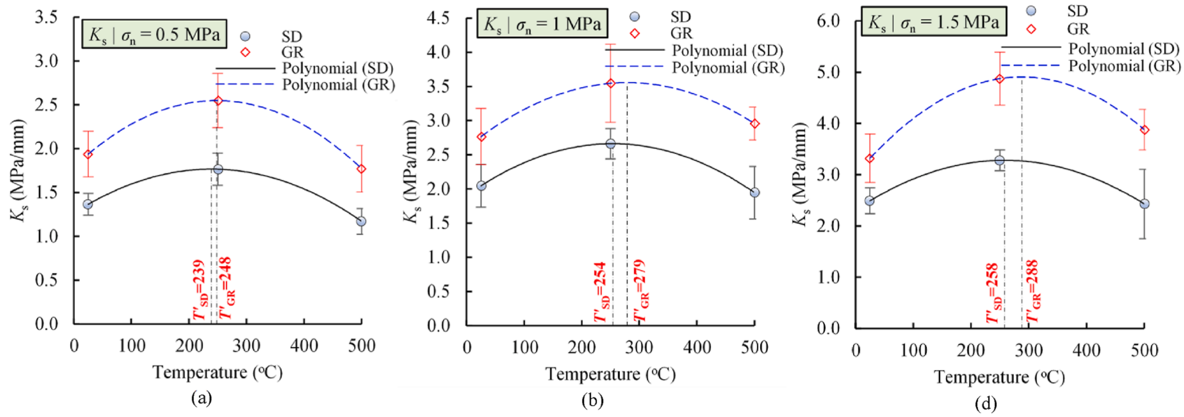

Fig. 13. The effect of thermal treatment on the shear stiffness under (a) σ_n = 0.5 MPa, (b) σ_n = 1 MPa, and (c) σ_n = 1.5 MPa.

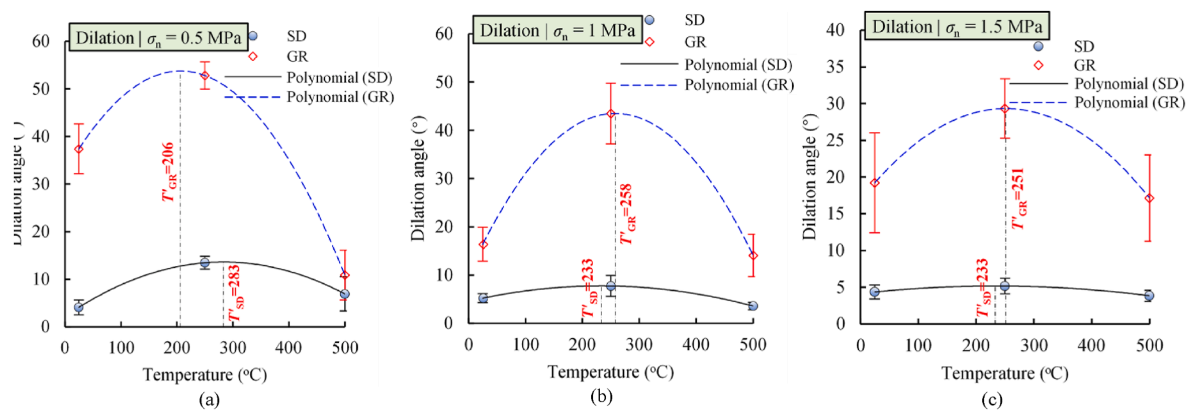

Fig. 14. The effect of thermal treatment on the dilation angle under (a) σ_n = 0.5 MPa, (b) σ_n = 1 MPa, and (c) σ_n = 1.5 MPa.

4.3. Failure envelope

Failure envelopes and equations that govern shear behavior in rock joints are important in rock mechanics, particularly for deep engineering projects that must consider environmental factors such as temperature. Several criteria describe the peak shear strength of joints as a function of the applied normal stress, such as the linear Mohr–Coulomb failure criterion, represented by the solid black line in Fig. 15a and b. However, the results show that the peak shear strength does not closely follow a linear relationship. Instead, the quadratic equation represented by the dashed red line in Fig. 15a and b more closely describes the relationship between τ_P and σ_n. Consequently, it is essential to develop a nonlinear model that captures the strength behavior of sandstone and granite joints, taking into account the effects of internal friction angle and cohesion. We found that Jaeger (1971)'s nonlinear model aligns well with the experimental results of sandstone and granite joints, as shown by the solid black line in Fig. 15c and d. Jaeger's failure envelope can be viewed as a smoothed approximation of Patton (1966)'s bilinear failure envelope, represented by the dashed red line in Fig. 15c and d. The model proposed by Jaeger (1971) is presented as follows:

$$\tau_P = c\left(1 - e^{-b\sigma_n}\right) + \sigma_n \tan \varphi \quad (5)$$

where b is an empirical constant; and c and φ are the cohesion and internal friction angle, respectively.

4.3.1. The effect of thermal treatment on failure envelope

To demonstrate the effect of thermal treatment on the failure envelopes of sandstone and granite joints, Fig. 16a displays all of Jaeger's failure envelopes for these joints under various temperature conditions. In addition, Fig. 16b–d shows experimental data alongside the analytical predictions of Patton and Jaeger at the same scale for temperatures at RT, 250 °C, and 500 °C, respectively. The failure envelopes of granite joints are consistently higher than those of sandstone joints across all temperature conditions. When the treatment temperature is increased to 250 °C (Fig. 16c), the failure envelopes for both sandstone and granite joints rise, with the difference between them widening. This indicates that the peak shear strength of granite joints improves more than that of sandstone joints after thermal treatment at this temperature. At 500 °C (Fig. 16d), however, the failure envelopes significantly deteriorate compared to the improvement observed at 250 °C. Furthermore, the gap between the failure envelopes of sandstone and granite joints narrows at 500 °C, suggesting that the thermal treatment at this higher temperature significantly reduces the peak shear strength of the rougher granite joints, making it comparable to that of the smoother sandstone joints.

Additionally, it should be noted that when using Patton's bilinear and Jaeger's nonlinear failure envelopes, the shear strength of rock joints can be described through two essential stages. The first stage is called the sliding stage and describes the sliding shear strength between joint surfaces under low normal stress that does not cause shearing of intact asperities. As the normal stress increases beyond a specific limit of approximately

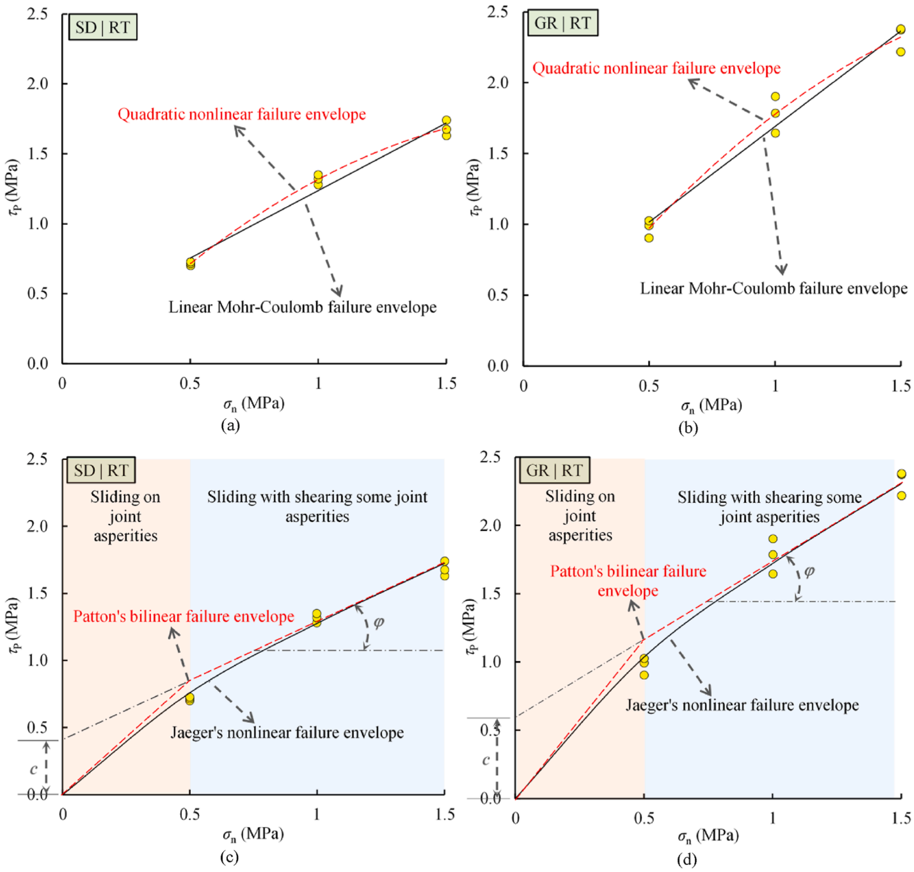

Fig. 15. Failure envelopes: (a, b) Linear and quadratic failure envelopes in sandstone and granite, respectively; and (c, d) Bilinear and nonlinear failure envelopes in sandstone and granite, respectively.

0.5 MPa at the three temperatures in our study, some intact asperities start to shear, and the slope of the τ_P-σ_n curve changes significantly. This marks the transition to the second stage, which involves sliding and shearing of some intact asperities. When the applied normal stress is high enough to shear all intact asperities, the second stage is called the shear stage.

4.3.2. The effect of thermal treatment on the cohesion and internal friction angle

Based on Jaeger's nonlinear failure envelope shown in Fig. 15, the internal friction angle (φ) can be determined from the slope of the linear portion of the failure envelope, which approximates the slope of the τ_P-σ_n curve during the second stage of sliding and shearing of some intact asperities. Cohesion is derived from the intersection of the linear part of the failure envelope with the τ_P axis. The effect of thermal treatment on the internal friction and cohesion of sandstone and granite joints is illustrated in Fig. 17a and b, respectively. Fig. 17a shows that the internal friction angle for granite joints is higher than that for sandstone joints under T = RT and 250 °C. However, after thermal treatment at 500 °C, the φ^{GR} becomes less than φ^{SR}, indicating that granite joints soften more than sandstone joints at this temperature. This softening explains the significant reduction in the granite's failure envelope after thermal treatment at 500 °C, making it nearly close to that of the sandstone (Fig. 16d). Despite this, the granite's failure envelope remains higher due to the cohesion effect, with Fig. 17b showing that the c^{GR} is approximately 80% greater than c^{SD}.

Furthermore, the internal friction angle and cohesion of granite joints behave in two regimes as the temperature increases from RT to 500 °C, with each parameter having a different threshold. This behavior is consistent with that observed in other studies investigating the effect of thermal treatment on the internal friction angle (Yang et al., 2022) and cohesion (Wang et al., 2024b). Although sandstone joints show a negligible threshold of the internal friction angle and cohesion at 473 °C and 131 °C, respectively, both parameters generally follow the same trend with increasing temperature from RT to 500 °C. The internal friction angle increases, while cohesion decreases with rising temperature. Li and Liu (2022) observed the same trend of treatment effect on intact sandstone: as the temperature increased from RT to 800 °C, the internal friction angle increased from about 34.5° to 43.8°, while the cohesion decreased from 16.5 MPa to 13 MPa.

5. Explanation and discussion of the observed results

Many researchers have reported that thermal treatment directly affects the rock's mineralogical and structural composition. Consequently, rocks can behave differently after exposure to heat. The physical and mechanical properties of rocks may change during or after thermal treatment due to various factors (Kumari et al., 2017; Tang et al., 2020; Orlander et al., 2021; Xu and Gong, 2021; Wong et al., 2022), the most important of which are physical and chemical interactions, differential mineral expansion, water evaporation, rock dehydration, and the generation and accumulation of microcracks. This study examined the effect of heat treatment on two rock types of different origins: granite, an igneous rock, and sandstone, a sedimentary rock. The mechanical properties of these two rocks at different temperatures are

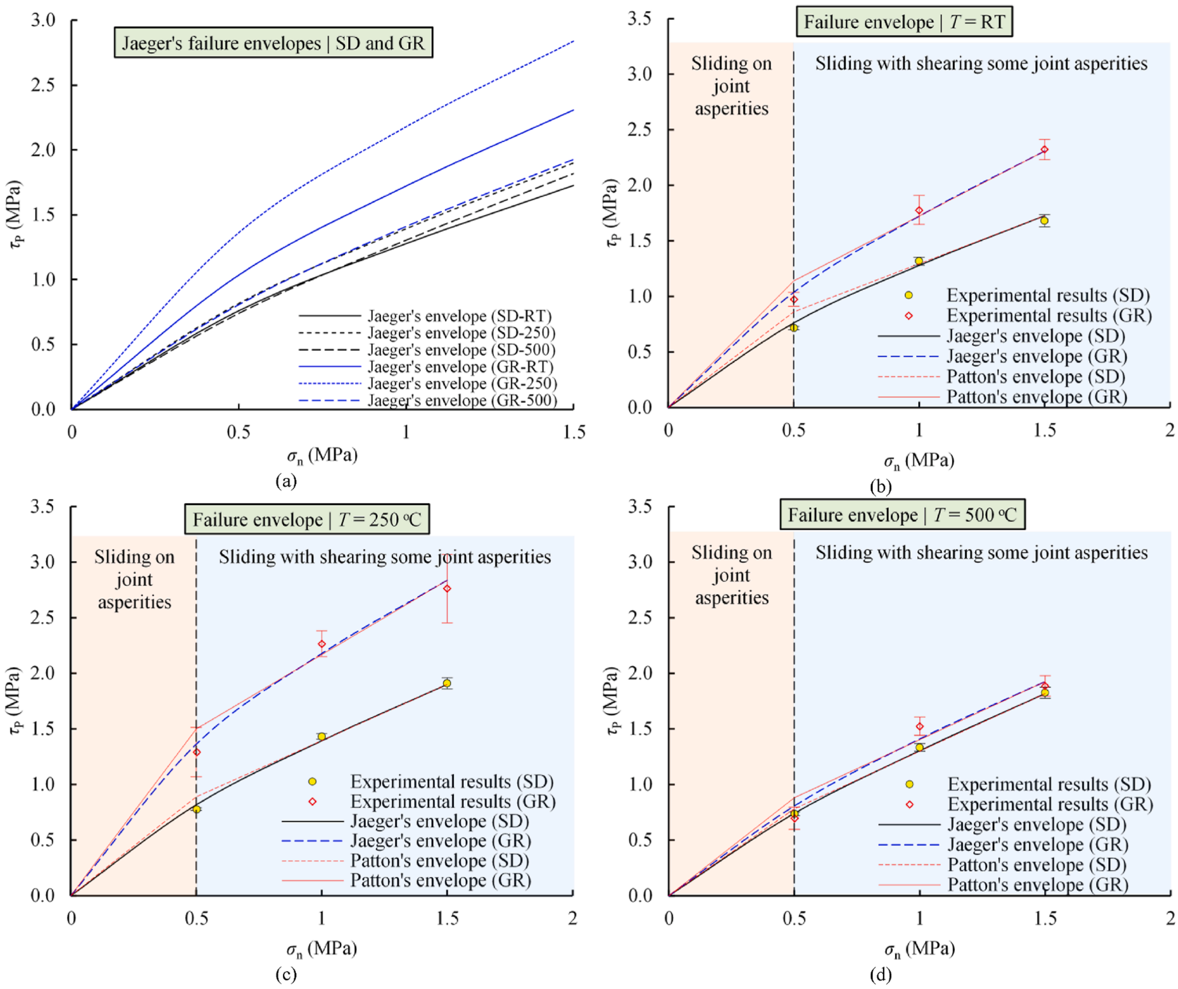

Fig. 16. (a) Jaeger's failure envelopes predicted in sandstone and granite joints; and experimental and analytical failure envelopes under (b) T = RT, (c) T = 250 °C, and (d) T = 500 °C.

quantitatively shown in Table 2. This table demonstrates that the joints of the two rock types exhibit nearly identical behavior under compression and shear loading, where the results align qualitatively but diverge quantitatively. The differences in the results and their implications can be discussed in terms of the mineralogical and structural composition of the two rocks. Analysis of the mineralogical composition indicated a high percentage of plagioclase and quartz in the two rock types. The sandstone contains 13% clay minerals, which have a high affinity for water and are sensitive to temperature changes. Granite, on the other hand, is characterized by a distinct structural composition due to natural cracks within and between the grains (intra- and inter-granular fractures). In addition, it was observed that the average grain size of the granite is 6.35 times greater than that of the sandstone,

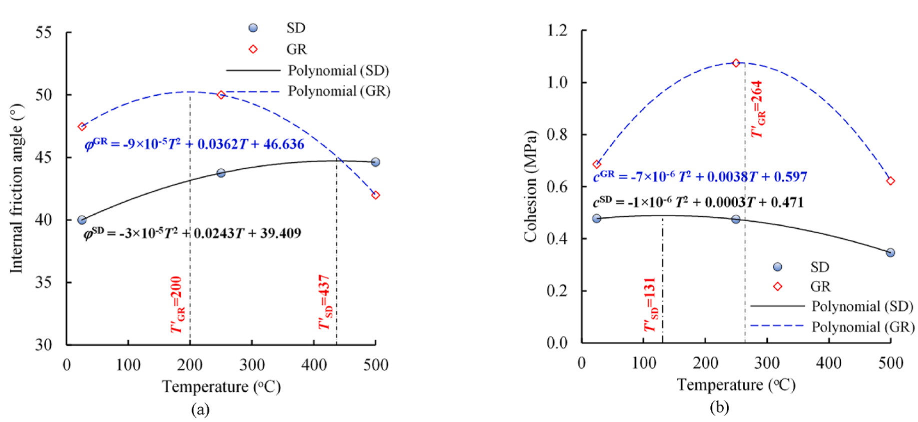

Fig. 17. The effect of thermal treatment on the (a) internal friction angle and (b) cohesion of sandstone and granite joints.

and the roughness coefficient of granite joints is 33.2% higher than that of the sandstone joints. Despite these differences, both rock types exhibit similar behavior as the temperature of thermal treatment increases from RT to 250 °C and 500 °C. An improvement in the behavior of sandstone and granite joints under compression and shear loading was observed as the temperature increased up to a threshold between 200 °C and 350 °C, followed by a deterioration beyond this threshold.

Many factors may contribute to the noticeable improvement in the behavior of sandstone and granite joints as the temperature increases up to a certain threshold. For instance, water evaporation is one of the most important factors leading to the noticeable improvement in rock behavior with increasing temperature. Yang et al. (2017) and Lei et al. (2019) concluded that weakly and strongly bound water can evaporate completely from sandstone structures at temperatures exceeding 150 °C and 200 °C, respectively. Wang et al. (2024a) demonstrated that bound and interlayer water can evaporate from granite as the temperature rises from RT to 400 °C. Water evaporation reduces the lubrication between joint surfaces, leading to increased friction and improved joint behavior under shearing (Li and Liu, 2022).

Additionally, the differential expansion of constituent minerals plays a vital role in improving the behavior of sandstone and granite joints with increasing temperature up to a certain threshold. Ding et al. (2016) observed that, at temperatures below 400 °C, the thermal expansion of internal mineral particles leads to the closure of the primary cracks, thereby reducing the number of cracks in sandstone samples. Wang et al. (2024a) observed a similar effect of thermal expansion on the shear behavior of granite fractures for the temperature range from RT to 400 °C. Therefore, as the temperature increases to a certain threshold, the relative volume of voids and pores and the width of the pre-existing fractures decrease in sandstone and granite. This increases the compactness of the global structure and the contact area between grains, thus improving the behavior of sandstone and granite joints under compression and shear.

Specifically, for sandstone, the presence of clay elements and calcite plays an important role in determining the behavior of this rock during/after thermal treatment due to the chemical reactions and transformations that occur in the minerals with increasing temperature. Desorption and decomposition of clay minerals in the sandstone can occur between 25 °C and 220 °C and 400 °C and 700 °C, respectively (Tian et al., 2012; Xiao et al., 2021). Li and Liu (2022) pointed out that the clay content in the sandstone drops sharply at T greater than 400 °C due to decomposition reaction. They also showed that the microstructure remains relatively unaffected by thermal treatment at temperatures below 400 °C. Beyond this temperature threshold, however, thermal cracks develop and the relative volume of pores increases, which explains the deterioration observed in the sandstone behavior when the temperature surpasses a certain threshold. Yang et al. (2017) reached a similar conclusion regarding the effect of temperature on sandstone microstructure. They showed that the average particle size increased by 350% as the temperature increased from RT to 300 °C, and then decreased by 30% within 300 °C-500 °C. This led to a reduction in the initial crack width with increasing temperature up to 300 °C, followed by an increase beyond this threshold.

The distinct structural composition of granite plays an important role in explaining its behavior under compression and shearing. Alneasan et al. (2022); Alneasan and Alzo'ubi (2022), and Kareem Alzo'ubi et al. (2024) investigated the effect of temperature on the same granite type at the three temperatures adopted in this study. They concluded that at RT, the grain boundaries are interlocked and in full contact. The fractures at RT appear with a relatively large width compared to the second case after thermal treatment at 250 °C. Following thermal treatment at 250 °C, the width of these fractures decreased due to water evaporation and differential mineral expansion, increasing the contact area between the fracture surfaces and improving granite behavior before a certain temperature threshold is exceeded. Following thermal treatment at 500 °C, many thermal fractures develop and coalesce, forming continuous large surfaces of weakness. This leads to a significant decline in the granite's behavior under compression and shearing as the temperature exceeds a certain threshold.

6. Conclusions

The effect of thermal treatment on the shear behavior of two types of sedimentary and igneous rocks, represented by sandstone and granite, respectively, was investigated. The focus was on the effect of temperature on the compressive and shear behavior of a single joint in these two types of rocks. A large number of artificial joints were created in prismatic samples of sandstone and granite. Finally, nine joints of each rock type were selected based on roughness conditions. Three samples of each rock type were thermally treated at 250 °C and three at 500 °C. Initially, the sandstone and granite joints were normally loaded up to 6 MPa to study the effect of temperature on the compressive behavior. Then, they were sheared under three constant normal stresses of

Table 2
The average values of the mechanical properties of sandstone and granite.

Property			Sandstone			Granite		
Temperature (°C)			RT	250	500	RT	250	500
Compressive behavior	δ_m (mm)		0.206	0.129	0.308	0.205	0.126	0.307
	K_{ni} (MPa/mm)		8.44	18.15	6.77	9.68	12.5	5.63
Shear behavior	τ_P (MPa)	$\sigma_n = 0.5$ MPa	0.714	0.776	0.737	0.973	1.291	0.696
		$\sigma_n = 1$ MPa	1.317	1.432	1.333	1.777	2.267	1.523
		$\sigma_n = 1.5$ MPa	1.682	1.911	1.827	2.322	2.762	1.886
	τ_R (MPa)	$\sigma_n = 0.5$ MPa	0.631	0.627	0.61	0.614	1.033	0.533
		$\sigma_n = 1$ MPa	1.191	1.107	1.13	1.478	1.993	1.143
		$\sigma_n = 1.5$ MPa	1.525	1.478	1.47	1.876	2.327	1.408
	K_s (MPa/mm)	$\sigma_n = 0.5$ MPa	1.365	1.765	1.171	1.937	2.549	1.771
		$\sigma_n = 1$ MPa	2.046	2.661	1.946	2.765	3.546	2.957
		$\sigma_n = 1.5$ MPa	2.49	3.279	2.428	3.319	4.873	3.876
	ψ (°)	$\sigma_n = 0.5$ MPa	4.1	13.5	6.9	37.4	52.8	10.9
		$\sigma_n = 1$ MPa	5.2	7.8	3.6	16.4	43.5	14.1
		$\sigma_n = 1.5$ MPa	4.4	5.2	3.8	19.2	29.3	17.1
	φ (°)		40	43.8	44.6	47.5	50	42
	c (MPa)		0.478	0.475	0.347	0.686	1.075	0.623

0.5 MPa, 1 MPa, and 1.5 MPa. The main conclusions of this study were as follows.

During the compression stage, the relationship between the applied normal stress and joint opening in both rocks adhered closely to a modified version of Bandis's equation, before and after thermal treatment. The maximum joint closure was very close for both rocks, reaching its minimum value at a temperature threshold of 215 °C. The initial normal stiffness of granite was greater than that of the sandstone, peaking at a temperature threshold of 215 °C and 253 °C in the granite and sandstone, respectively.

During the shear stage, the results showed a noticeable improvement in the shear behavior of sandstone and granite joints as the temperature increased to a threshold of 200 °C-350 °C, followed by deterioration once this threshold was exceeded. The shear strength parameters of granite, including peak and residual shear strength, shear stiffness, dilation angle, internal friction angle and cohesion, were generally greater than those of sandstone. In addition, the relationship between the applied normal stress and peak shear strength was approximately nonlinear for the two rock types, resulting in nonlinear failure envelopes before and after thermal treatment. Consequently, it was found that the peak shear strength followed Patton's bilinear failure criterion and Jaeger's nonlinear criterion more closely than the Mohr–Coulomb linear criterion. These findings are important for enhancing the safety and design of geothermal energy systems and deep underground constructions, where rocks are subjected to high temperatures. Future research should examine the effects of cyclic thermal treatments on more rock types to better simulate real-world circumstances involving geothermal and subsurface engineering.

CRediT authorship contribution statement

Abdel Kareem Alzo'ubi: Software, Resources, Methodology, Formal analysis, Writing – original draft, Project administration, Funding acquisition, Conceptualization, Visualization, Supervision, Data curation, Writing – review & editing, Validation, Investigation. **Mahmoud Alneasan:** Formal analysis, Data curation, Validation, Investigation, Writing – review & editing, Resources, Visualization, Conceptualization, Software, Writing – original draft, Methodology.

Declaration of competing interest

The authors declare that they have no known competing financial interests or personal relationships that could have appeared to influence the work reported in this paper.

Acknowledgment

We would like to thank the ORSP at Abu Dhabi University, UAE, for funding this project (Grant No. 19300751).

References

Akhavan, A., Rajabipour, F., 2012. Quantifying the effects of crack width, tortuosity, and roughness on water permeability of cracked mortars. Cement Concr. Res. 42, 313–320.

Alneasan, M., Alzo'ubi, A.K., 2022. Comprehensive investigation of rock fracture behaviour in clay-rich rocks under the effect of temperature: experimental study under three loading modes (I, I/II, II). Eng. Fract. Mech. 276, 108933.

Alneasan, M., Alzo'ubi, A.K., Behnia, M., Mughieda, O., 2022. Experimental observations on the effect of thermal treatment on the crack speed and mode I and II fracture toughness in brittle and ductile rocks. Theor. Appl. Fract. Mech. 121, 103525.

Alneasan, M., Alzo'ubi, A.K., 2022. Temperature effect on the fracture behavior of granite under three loading modes (I, I/II, and II). Rock Mech. Rock Eng. 56, 1–15.

Alneasan, M., Alzo'ubi, A.K., 2023. Extensive experimental investigation on the effect of thermal treatment and lateral pressure on the shear behavior of intact mudstone. Sci. Rep. 13, 6820.

Alzo'ubi, A.K., Alneasan, M., 2022. Experimental study on the effect of thermal treatment on the mechanical properties of clay-rich rocks (mudstone). Results Eng. 16, 100728.

Alzo'ubi, A.K., Alneasan, M., Ibrahim, F., 2024. The mechanical behavior of mudstone under coupling effect of temperature and confining pressure: a comprehensive investigation. Rock Mech. Rock Eng. 57, 2325–2338.

ASTM D5067–16, 2021. Standard Specification for Artists' Watercolor Paints. West Conshohocken, USA.

Bandis, S., Lumsden, A., Barton, N., 1983. Fundamentals of rock joint deformation. Int. J. Rock Mech. Min. Sci. Geomech. Abstr. 20 (6), 249–268.

Bi, J., Du, C., Zhao, Y., Wang, C., Lian, S., Xiong, X., 2023. Characterization of shear behavior and damage mechanism of periodic thermal loading sandstone based on NMR technique. Eng. Geol. 325, 107272.

Boggs, S., 2011. Principles of Sedimentology and Stratigraphy, fifth ed. Pearson, Harlow, UK.

Chen, B., Shen, B., Jiang, H., 2023. Shear behavior of intact granite under thermo-mechanical coupling and three-dimensional morphology of shear-formed fractures. J. Rock Mech. Geotech. Eng. 15 (3), 523–537.

Chen, Y., Zhang, C., Zhao, Z., Zhao, X., 2020. Shear behavior of artificial and natural granite fractures after heating and water-cooling treatment. Rock Mech. Rock Eng. 53, 5429–5449.

Ding, Q.-L., Ju, F., Mao, X.B., Ma, D., Yu, B.Y., Song, S.B., 2016. Experimental investigation of the mechanical behavior in unloading conditions of sandstone after high-temperature treatment. Rock Mech. Rock Eng. 49, 2641–2653.

Fraser, H., 1986. Ceramic Faults and Their Remedies. A&C Black, London, UK.

Griffiths, L., Heap, M., Baud, P., Schmittbuhl, J., 2017. Quantification of microcrack characteristics and implications for stiffness and strength of granite. Int. J. Rock Mech. Min. Sci. 100, 138–150.

Hudson, J.A., Stephansson, O., Andersson, J., Tsang, C.F., Jing, L., 2001. Coupled T–H–M issues relating to radioactive waste repository design and performance. Int. J. Rock Mech. Min. Sci. 38, 143–161.

Jaeger, J., 1971. Friction of rocks and stability of rock slopes. Geotechnique 21, 97–134.

Jiang, T., Chen, B., Zhang, Q., Bai, J., Li, W., 2024. Thermal stimulation mechanical response and shear dilatation predictive model improvement of granite fractures in an enhanced geothermal system. J. Mater. Res. Technol. 28, 4334–4349.

Johnson, B., Gangi, A., Handin, J., 1978. Thermal cracking of rock subjected to slow, uniform temperature changes. In: The 19th U.S. Symposium on Rock Mechanics (USRMS), Reno, USA. Paper No. ARMA-78-0318.

Kareem Alzo'ubi, A., Alneasan, M., Ibrahim, F., Okasha, N.M., Mirrashid, M., 2024. Thermal treatment effects on rock fracture behaviour under three loading modes: a comparative analysis of granite and mudstone. Eng. Fail. Anal. 159, 108092.

Kumari, W.G.P., Ranjith, P.G., Perera, M.S.A., Chen, B.K., Abdulagatov, I.M., 2017. Temperature-dependent mechanical behaviour of Australian Strathbogie granite with different cooling treatments. Eng. Geol. 229, 31–44.

Lei, R., Wang, Y., Zhang, L., Liu, B., Long, K., Luo, P., Wang, Y., 2019. The evolution of sandstone microstructure and mechanical properties with thermal damage. Energy Sci. Eng. 7, 3058–3075.

Li, M., Liu, X., 2022. Effect of thermal treatment on the physical and mechanical properties of sandstone: insights from experiments and simulations. Rock Mech. Rock Eng. 55, 3171–3194.

Liu, K., Huang, X., Zhang, S., Guo, T., Ma, S., Zhou, Z., 2022. Effects of thermal treatment on the shear behavior and characteristics of intact sandstone: laboratory experiment of variable-angle shear. Bull. Eng. Geol. Environ. 81, 471.

Liu, S., Li, S.C., Liu, R.C., Yu, L.Y., Wang, Y.S., 2023. Experimental study on the evolutions of normal stiffness of fractured granites after different temperature treatments. J. Cent. South Univ. 30, 488–502.

Lu, Y., Wang, L., Sun, X., Wang, J., 2017. Experimental study of the influence of water and temperature on the mechanical behavior of mudstone and sandstone. Bull. Eng. Geol. Environ. 76, 645–660.

Ma, X., Wang, G., Hu, D., Liu, Y., Zhou, H., Liu, F., 2020. Mechanical properties of granite under real-time high temperature and three-dimensional stress. Int. J. Rock Mech. Min. Sci. 136, 104521.

Meng, F., Wong, L.N.Y., Zhou, H., 2021. Rock brittleness indices and their applications to different fields of rock engineering: a review. J. Rock Mech. Geotech. Eng. 13, 221–247.

Meng, Q.B., Qian, W., Liu, J.F., Zhang, M.W., Lu, M.M., Wu, Y., 2020. Analysis of triaxial compression deformation and strength characteristics of limestone after high temperature. Arabian J. Geosci. 13, 153.

Nasseri, M.H.B., Schubnel, A., Young, R.P., 2007. Coupled evolutions of fracture toughness and elastic wave velocities at high crack density in thermally treated Westerly granite. Int. J. Rock Mech. Min. Sci. 44, 601–616.

Orlander, T., Andreassen, K.A., Fabricius, I.L., 2021. Effect of temperature on stiffness of sandstones from the deep North Sea Basin. Rock Mech. Rock Eng. 54, 255–288.

Pan, J., Zhang, Y., Li, P., Wu, X., Xi, X., 2023. Mechanical properties and thermo-chemical damage constitutive model of granite subjected to thermal and chemical treatments under uniaxial compression. Constr. Build. Mater. 390, 131755.

Patton, F.D., 1966. Multiple Modes of Shear Failure in Rock and Related Materials. University of Illinois at Urbana-Champaign, Urbana, USA. PhD Thesis.
Rathnaweera, T.D., Ranjith, P.G., Gu, X., et al., 2018. Experimental investigation of thermomechanical behaviour of clay-rich sandstone at extreme temperatures followed by cooling treatments. Int. J. Rock Mech. Min. Sci. 107, 208–223.
Rice, J., 1996. Low-stress faulting: strong but brittle faults with local stress concentrations. Eos Trans. Am. Geophys. Union 77, F471.
Rimi, A., Zarhloule, Y., Barkaoui, A.E., Correia, A., Carneiro, J., Verdoya, M., Lucazeau, F., 2012. Towards a de-carbonized energy system in north-eastern Morocco: prospective geothermal resource. Renew. Sustain. Energy Rev. 16, 2207–2216.
Singh, B., Cattle, S.R., Field, D.J., 2014. Edaphic soil science, introduction to. In: Van Alfen, N.K. (Ed.), Encyclopedia of Agriculture and Food Systems. Academic Press, Oxford, UK, pp. 35–58.
Su, H., Nie, Y., Feng, Y., Yu, L., Chen, G., Wang, W., 2022. Experimental investigation on microstructure characteristics and deformation failure behaviors of sandstone after high temperature under Brazilian splitting. Geomech. Geophys. Geo-Energy Geo-Resour. 8, 121.
Tang, Z.C., 2020. Experimental investigation on temperature-dependent shear behaviors of granite discontinuity. Rock Mech. Rock Eng. 53, 4043–4060.
Tang, Z.C., Sun, M., Peng, J., 2019. Influence of high temperature duration on physical, thermal and mechanical properties of a fine-grained marble. Appl. Therm. Eng. 156, 34–50.
Tang, Z.C., Zhang, Q.Z., Peng, J., 2020. Effect of thermal treatment on the basic friction angle of rock joint. Rock Mech. Rock Eng. 53, 1973–1990.
Tian, H., Kempka, T., Xu, N.X., Ziegler, M., 2012. Physical Properties of sandstones after high temperature treatment. Rock Mech. Rock Eng. 45, 1113–1117.
Wang, D., Ma, Y., Liu, X., Li, D., Liu, Q., Yang, H., Li, X., 2024b. Improving mining sustainability and safety by monitoring precursors of catastrophic failures in loaded granite: an experimental study of acoustic emission and electromagnetic radiation. Sustainability 16, 1045.
Wang, P., Wang, C., Wang, G., Jiang, Y., Xu, F., 2024a. Experiment study on shear behavior and properties of granite fractures under real-time high-temperature conditions. Geomech. Energy Environ. 38, 100539.
Wong, L.N.Y., Cui, X., Zhang, Y., Wu, Z., Guo, T., 2022. Experimental investigation of thermal strengthening in Sichuan marble. Rock Mech. Rock Eng. 55, 6683–6702.
Xiao, W., Yu, G., Li, H., Zhan, W., Zhang, D., 2021. Experimental study on the failure process of sandstone subjected to cyclic loading and unloading after high temperature treatment. Eng. Geol. 293, 106305.
Xu, L., Gong, F., 2021. Experimental study of strain rockburst considering temperature effect: status-of-the-art and prospect. Shock Vib. 2021, 8767592.
Yang, J., Fu, L.Y., Wang, F., Deng, W., 2022. Coupled thermo–mechanical damage evolution of granite under repeated heating–cooling cycles and the applications of Mohr–Coulomb and Drucker–Prager models. Nat. Resour. Res. 31, 2629–2652.
Yang, S.Q., Xu, P., Li, Y.B., Huang, Y.H., 2017. Experimental investigation on triaxial mechanical and permeability behavior of sandstone after exposure to different high temperature treatments. Geothermics 69, 93–109.
Yin, Q., Wu, J., Zhu, C., He, M., Meng, Q., Jing, H., 2021. Shear mechanical responses of sandstone exposed to high temperature under constant normal stiffness boundary conditions. Geomech. Geophys. Geo-Energy Geo-Resour. 7, 35.
Zhai, T., Zhu, J., Zhou, C., Yang, T., 2022. Experimental investigation of the effect of thermal treatment on shear characteristics of healed rock joints. Int. J. Rock Mech. Min. Sci. 152, 105074.
Zhang, F., Zhao, J., Hu, D., Skoczylas, F., Shao, J., 2018. Laboratory investigation on physical and mechanical properties of granite after heating and water-cooling treatment. Rock Mech. Rock Eng. 51, 677–694.
Zhang, Q., Li, X., Bai, B., Hu, H., 2019. The shear behavior of sandstone joints under different fluid and temperature conditions. Eng. Geol. 257, 105143.
Zhang, W., Sun, Q., Zhu, S., Wang, B., 2017. Experimental study on mechanical and porous characteristics of limestone affected by high temperature. Appl. Therm. Eng. 110, 356–362.
Zhao, Z., Dou, Z., Xu, H., Liu, Z., 2019. Shear behavior of Beishan granite fractures after thermal treatment. Eng. Fract. Mech. 213, 223–240.
Zhou, H., Liu, Z., Liu, F., Shao, J., Li, G., 2024. Anisotropic strength, deformation and failure of gneiss granite under high stress and temperature coupled true triaxial compression. J. Rock Mech. Geotech. Eng. 16, 860–876.
Zhu, Z., Tian, H., Kempka, T., Jiang, G., Dou, B., Mei, G., 2021. Mechanical behaviors of granite after thermal treatment under loading and unloading conditions. Nat. Resour. Res. 30, 2733–2752.